PLOS BIOLOGY

RESEARCH ARTICLE

Entorhinal transformations in abstract frames of reference

Raphael Kaplan[1,2]*, **Karl J. Friston**[1]

1 Wellcome Centre for Human Neuroimaging, UCL Queen Square Institute of Neurology, University College London, London, United Kingdom, **2** Egil and Pauline Braathen and Fred Kavli Centre for Cortical Microcircuits, Kavli Institute for Systems Neuroscience, Norwegian University of Science and Technology, Trondheim, Norway

* raphael.s.m.kaplan@ntnu.no

Citation: Kaplan R, Friston KJ (2019) Entorhinal transformations in abstract frames of reference. PLoS Biol 17(5): e3000230. https://doi.org/10.1371/journal.pbio.3000230

Academic Editor: Matthew F. S. Rushworth, Oxford University, UNITED KINGDOM

Received: February 14, 2019

Accepted: March 29, 2019

Published: May 2, 2019

Data Availability Statement: Quantitative data for all X-Y and bar plots are included in the Supporting Information. Neural data is available at Figshare public repository (URL: https://figshare.com/articles/Kaplan_Friston2019PLoSBiologyNeuralData_zip/7844495 DOI: https://doi.org/10.6084/m9.figshare.7844495.v1).

Funding: This research was supported by grants from the Wellcome Trust (https://wellcome.ac.uk/) to RK (grant number 101261/Z/13/Z), KJF (grant number 088130/Z/09/Z), and the Wellcome Centre for Human Neuroimaging (grant number 203147/

Abstract

Knowing how another's preferences relate to our own is a central aspect of everyday decision-making, yet how the brain performs this transformation is unclear. Here, we ask whether the putative role of the hippocampal–entorhinal system in transforming relative and absolute spatial coordinates during navigation extends to transformations in abstract decision spaces. During functional magnetic resonance imaging (fMRI), subjects learned a stranger's preference for an everyday activity—relative to one of three personally known individuals—and subsequently decided how the stranger's preference relates to the other two individuals' preferences. We observed entorhinal/subicular responses to the absolute distance between the ratings of the stranger and the familiar choice options. Notably, entorhinal/subicular signals were sensitive to which familiar individuals were being compared to the stranger. In contrast, striatal signals increased when accurately determining the ordinal position of choice options in relation to the stranger. Paralleling its role in navigation, these data implicate the entorhinal/subicular region in assimilating relatively coded knowledge within abstract metric spaces.

Introduction

Learning other people's attributes is facilitated by expressing personal preferences ordinally—whether we prefer one thing to another—and metrically—how much more we prefer one thing over another. Ordinal and metric coding are particularly important when acquiring knowledge about new people. This type of learning involves relating a new person's attributes to prior beliefs about other people, either by adopting a relative or absolute frame of reference. For instance, imagine you are preparing dinner for a foreign visitor who says, "I like spicy food." If they are Vietnamese, their preference for spicy food is probably greater than Germanic tastes despite everyone declaring the same preference.

On one hand, progress has been made in linking the hippocampus to the maintenance of an ordinal sequence or "hierarchy" of personal attributes [1–5] and, similarly, category learning [6–8]. Yet the neural representation of metrically coded knowledge remains elusive, even

Z/16/Z). The funder had no role in study design, data collection and analysis, decision to publish, or preparation of the manuscript.

Competing interests: The authors have declared that no competing interests exist.

Abbreviations: BIC, Bayesian information criterion; fMRI, functional magnetic resonance imaging; FWE, family-wise error; ITI, intertrial interval; PPC, posterior parietal cortex; RT, reaction time; SPL, superior parietal lobule.

though metric coding affords the transformation of knowledge learned via relative and absolute frames of reference.

Clues about the neural computations underlying the transformation of abstract knowledge among frames of reference may come from research on the role of the hippocampal formation in path integration: the process of calculating one's position by estimating the direction and distance one has traveled from a known point. During path integration, specific subregions of the hippocampal formation have been implicated in integrating relative and absolute spatial coordinates during navigation in order to reach a desired location [9]. In particular, grid cells in entorhinal/subicular areas are selectively active at multiple spatial scales when an animal encounters periodic triangular locations covering the entire environment [10–11], while hippocampal place cells code specific locations in an environment [12]. Working together with boundary vector cells in entorhinal/subicular areas—that code an environmental boundary at a particular direction and distance [13–15]—and head direction cells [16], spatially modulated neurons in the hippocampal formation are thought to serve collectively as a cognitive map of the environment [17–18].

Notably, recent findings have extended the idea of map-like coding in the entorhinal cortex and subiculum to humans. Human entorhinal/subicular regions respond to both the distance of goal locations [19–20] and discrete abstract relations [21], suggesting that entorhinal/subicular areas might represent abstract knowledge metrically along multiple dimensions. Taken together, these results imply that neural computations in the hippocampal formation related to spatial exploration may also underlie the integration of information learned in different reference frames during more abstract types of memory-guided decision-making [22].

We investigated whether specific brain regions, including subregions of the hippocampal formation—like the entorhinal/subicular area—facilitate switching between different relative and absolute reference frames during memory-guided decisions. To test this hypothesis, we developed a novel experimental task, for which healthy volunteers were first asked to rate 1–9, on a 0–10 scale, how likely (likelihood) they (self), a close friend (friend), and a typical person (canonical) were to partake in a variety of everyday scenarios (e.g., eat spicy food, read a book, cycle to work; Fig 1A). To allow for strangers with more extreme ratings than the familiar individuals in the functional magnetic resonance imaging (fMRI) paradigm, subjects were restricted to rating between 1–9. Subsequently, subjects performed a forced-choice fMRI task (Fig 1B), for which they judged the proximity of a stranger's rating relative to the ratings of the self, friend, and canonical individuals for a given everyday scenario (Fig 1B). Specifically, on each (self-paced) trial, subjects were shown the preference of a stranger on a 0–10 scale, relative to a known person (anchor) and subjects had to select which of the two remaining (nonanchor) familiar individuals were closest to the stranger. After making a decision, a jittered (mean = 2.43 s) intertrial interval (ITI) period started, during which a white fixation point overlaid on a black background appeared on the screen.

In our task, it was crucial that the anchor was always placed in the middle of the scale to ensure that subjects used their prior knowledge in order to infer the stranger's absolute preference and form an appropriate mental number line of personal preferences (i.e., remembering the absolute positions of the different preferences on the number line instead of the visible relative position of the anchor in the middle of the screen with a stranger presented somewhere between 0–10; see Fig 1C and 1D). In other words, subjects had to infer the stranger's position in relation to the anchor's "true" rating for that scenario (i.e., the rating they gave for that anchor and scenario during the training period) and mentally rescale this information relative to the closest boundary (0 or 10). Note that this is a nontrivial task because the preferences of strangers were not conserved over attributes.

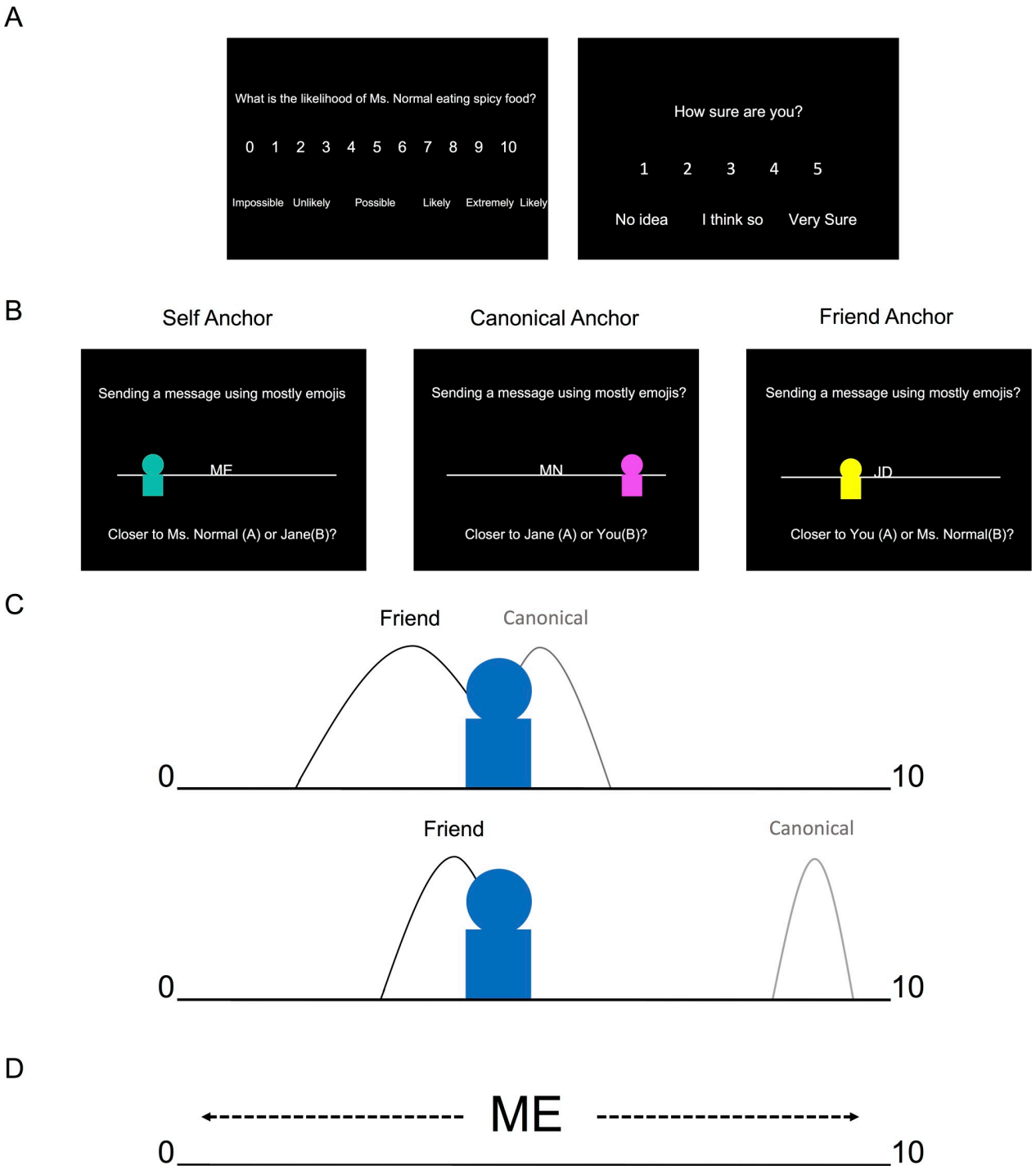

Fig 1. Experiment. A. Right before fMRI scanning, subjects were instructed to choose a friend with a different personality of the same gender. Subsequently, subjects rated from 1–9, on a 0–10 scale, how likely (likelihood) they (self), a close friend (friend), and the typical person (canonical) were to partake in a variety of everyday scenarios (e.g., eat spicy food, read a book, cycle to work). To allow for strangers with more extreme ratings than the familiar individuals in the fMRI paradigm, subjects were restricted to rating between 1–9. Subjects also reported their confidence, on a 1–5 scale, for each scenario. B. fMRI paradigm. During a forced-choice task, subjects made a decision on the relative proximity of a stranger's likelihood rating for an everyday scenario relative to the likelihood ratings for the self, friend, and canonical individuals for that same scenario. On each self-paced trial (max. allowed response time 9 s), subjects viewed a personal preference for a new stranger presented relative to one of the known individuals' initials (anchor) on a number line. Subjects had to determine which one of the two remaining (i.e., nonanchor) familiar individuals was closer to the stranger's rating. Crucially, the anchor individual (e.g., ME = self; MN = canonical "Mr./Ms. Normal;" JD = friend's initial) was always placed in the middle of the scale, ensuring that subjects had to use memory of their ratings made before fMRI scanning to infer the stranger's

absolute preference relative to the anchor's true rating and the ends of the number line. Additionally, subjects were instructed that the number line ranged from 0 and 10. For example, if the stranger was three-fourths to the right of the anchor with a rating of 9, the participant would infer that the stranger's rating was three-fourths of the way between 9 and 10 (the right boundary of the scale). Consequently, the participant would indicate that the stranger's rating would be approximately near 10. Notably, the numbers on the scale were not visible during the task. After making a decision, an intertrial interval (mean = 2.43 s) screen with a white fixation point in the center of a black screen appeared. C. Illustration of the behavioral model. Top illustration shows an ambiguous, less discriminable choice, while the bottom illustration shows a straightforward, highly discriminable choice. We quantified the difficulty of discriminating a particular choice by fitting a formal signal detection model, based on the absolute distance between the two choice individuals on the scale and how confident subjects were in their ratings (e.g., comparing the stranger's rating, represented by the blue avatar, with their rating for their friend and the canonical individual). Subjective confidence was represented by the standard deviation for each rating (e.g., curve width in the illustrations), where lower confidence entails higher standard deviations, and helped account for the influence of memory on choice behavior. D. Anchor rescaling. Illustration of how the stranger's rating is inferred by mentally rescaling the anchor individual's rating from its perceived relative position on the screen (5), to its absolute position (participant's rating) on the preference scale. fMRI, functional magnetic resonance imaging.

https://doi.org/10.1371/journal.pbio.3000230.g001

In summary, training subjects to think of absolutely coded personal preferences in the form of a mental number line allowed us to probe different everyday scenarios at various levels of discriminability and to use a well-characterized signal detection model of decision-making [23]. Discriminability was determined by the absolute distance between individuals on a scale and how confident subjects were about a particular preference. Furthermore, this modeling approach allowed us to quantify the differing mnemonic demands related to the subject knowing their ratings better for themselves (self) than their friend and canonical ratings (Fig 1C). Casting our paradigm in terms of coordinate transformations, we investigated how personal preferences learned via different anchors are differentially represented in the brain in two complementary ways: first, how the stranger's rating is inferred by mentally rescaling the anchor individual's rating from its perceived relative position on the screen to its absolute position (the participant's actual rating) on the preference scale (i.e., anchor rescaling). Second, uncertainty in preference discrimination based on the absolute distance between the stranger's rating and the ratings of the personally familiar individuals that the stranger is compared with (i.e., choice discriminability). We subsequently refer to these two elements of representing personal preferences in our task as anchor rescaling (Fig 1D) and choice discriminability (Fig 1C), respectively.

Results

Behavior

Subjects' ratings of personally known individuals followed a consistent structure. As expected, subjects tended to rate the canonical individual toward the middle of the scale, 5, with the self and friend ratings being more evenly dispersed between 1–9 (Fig 2A). Subjects' ratings for the canonical exemplar and their friend were generally consistent before and after scanning; after scanning, subjects were on average within ±1 of their original ratings for 67.7% (SD = 8.15%) of trials and only made large deviations from their original ratings > = ±3 on 8.54% (SD = 6.2%) of occasions (Fig 2B). Notably, there was a significant effect of anchor condition (self, canonical, or friend) for the average absolute distance between the choice options and the stranger ($F[2,22] = 10.1$; $P = 0.001$), for which self (mean = 2.34; SD = 0.412) and friend (mean = 2.26; SD = 0.371) anchor conditions had significantly smaller absolute distances than the canonical (mean = 2.62; SD = 0.473) anchor condition (Fig 2C). Unsurprisingly, we observed that there was an effect of anchor condition for subjective confidence ratings ($F[2,22] = 74.0$; $P < 0.001$), for which subjects were more confident about anchor conditions involving decisions with self-comparisons. Additionally, there were overlapping ratings (the same rating for two individuals on the same scenario) for a small subset of preferences, and there was a significant effect of anchor condition in the number of overlapping ratings ($F[2,22] = 6.74$;

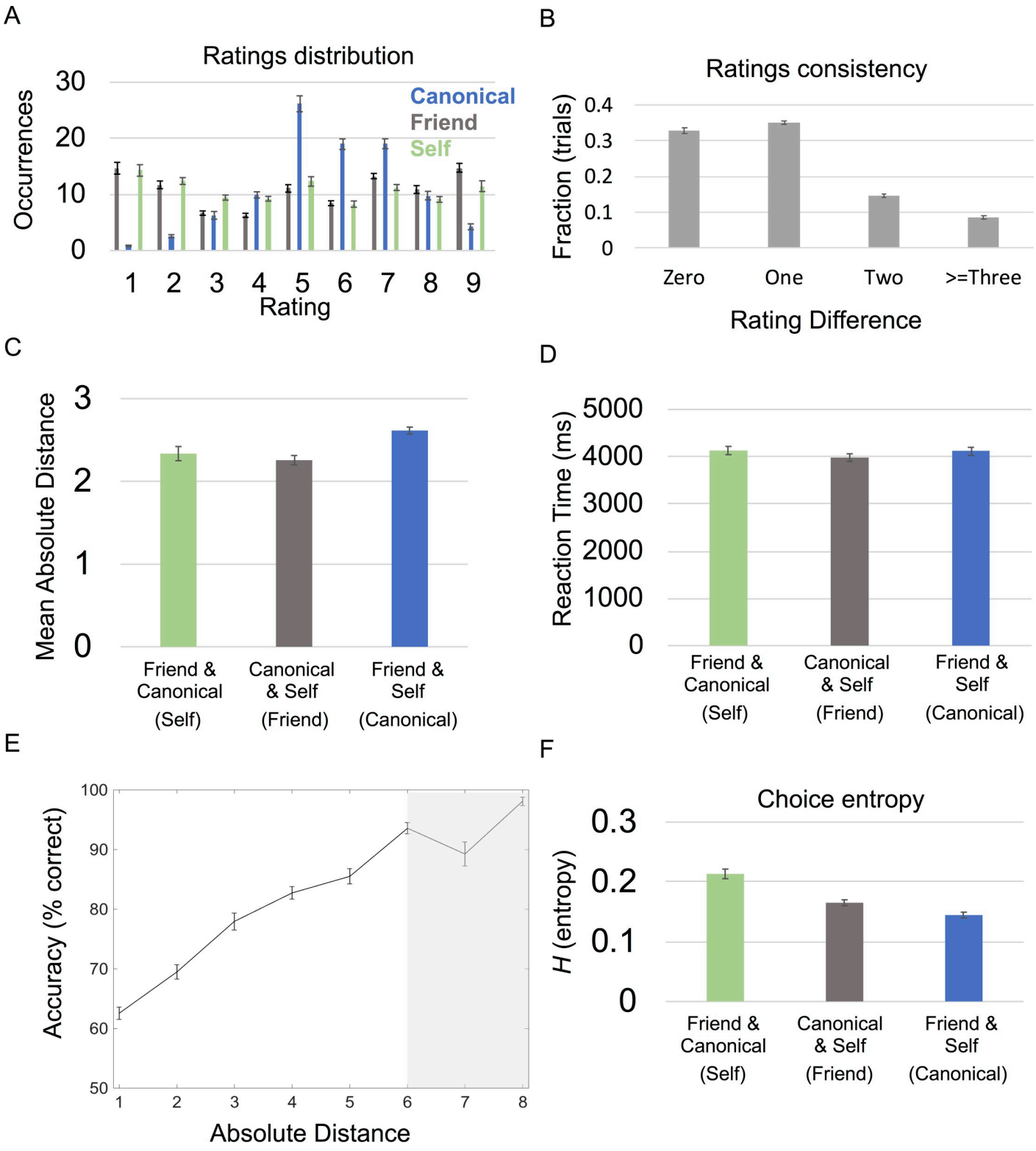

Fig 2. Behavioral results. A. Mean ratings across subjects for each familiar individual and every scenario. Occurrences are out of the 100 total trials per condition. B. Rating consistency. Difference in ratings pre- and post-fMRI scanning for friend and canonical individuals C. Distribution of mean absolute distances by condition. Significant effect of condition for absolute distance between the two individuals' ratings and the stranger's ($P = 0.001$). Individuals being compared are listed in the key with the corresponding anchor/condition name listed in parentheses. D. Reaction time: Significant effect of condition for reaction time/decision speed ($P = 0.022$). Individuals being compared are listed below each bar with the corresponding anchor condition listed in parentheses. E. Absolute distances and

performance. Significant relationship ($P < 0.001$) between accuracy and the absolute distance between strangers' ratings and the nonanchor individuals for each trial. 50% represents chance level of accuracy. Seven and 8 on the x-axis are shaded in gray because 18/24 and 13/24 of subjects had trials with absolute distances of 7 and 8, respectively. F. Choice entropy: Significant effect of condition for choice entropy ($P < 0.001$). Individuals being compared listed below each bar, with corresponding anchor listed in parentheses. All error bars showing mean ± SEM. For absolute distance plots, the absolute value of each absolute distance was rounded to the closest integer and plotted from 1 to 8. See S1 Data for subject data. fMRI, functional magnetic resonance imaging.

https://doi.org/10.1371/journal.pbio.3000230.g002

$P = 0.005$), such that there was higher overlap between self and friend ratings (the canonical anchor condition) than between other pairings (S1 Fig). Crucially, trials with overlapping ratings were always considered correctly answered and not included in subsequent behavioral and fMRI analyses. When relating subjective confidence to rating consistency, confidence ratings significantly correlated with rating consistency (t[23] = -4.11; $p < 0.001$), for which higher confidence ratings had more rating consistency. These results suggest a metacognitive validity of the subjective ratings, relating to memory for specific personal preferences.

During the fMRI experiment, subjects made 72.6% of decisions correctly (SD = 1.13%; $n = 24$), after eliminating trials for which either answer was correct (i.e., same or equidistant ratings). The mean reaction time (RT) was 4.07 s (SD = 0.803 s). There was a significant effect of condition ($P < 0.05$) for RT (F[2,22] = 4.57; $P = 0.022$; Fig 2D) but not performance (F[2,22] = 2.73; $P = 0.087$). The RT effect was driven by significantly higher RT for self versus friend anchor conditions (t[23] = 2.71; $P = 0.012$; Fig 2D). Notably, there was a negative correlation between trial by trial RT and accuracy (t[23] = -5.51; $P < 0.001$), i.e., quicker RT for accurate choices. In parallel, RT and rating consistency were also correlated (t[23] = 2.55; $P = 0.015$), where slower RT related to trials containing inconsistently rated preferences (i.e., poorly remembered preferences),

We then related RT and accuracy to the absolute distance between the stranger's rating and the ratings of the nonanchor individuals presented as choice options for each trial (i.e., choice discriminability without the use of a model and confidence ratings). As expected, we found that this distance negatively correlated with RT (t[23] = -5.42; $P < 0.001$) and positively correlated with accuracy (t[23] = 15.8; $P < 0.001$); i.e., larger distances related to quicker and more accurate decisions. Highlighting how the metric nature of these absolute distances influenced behavior, we observed a steady increase in the quickness (S2 Fig) and accuracy (Fig 2E) of the participant's responses when the stranger's rating was closer to one choice option versus another. Further relating these absolute distances to subjects' behavior, we then used a signal detection model fit to subjects' performance that was based on absolute rating distances and subjective confidence ratings. Given the relationship between subjective confidence and rating consistency, subjective confidence ratings also helped account for the different mnemonic demands induced by the different conditions.

A computational model of latent preferences. We quantified the difficulty of discriminating a particular preference by fitting a formal signal detection model [23] based on the absolute distance between the two choice (nonanchor) individuals on a scale and subjective confidence. Specifically, we characterized discriminability using the entropy of decision probabilities based on a softmax function of likelihood and confidence ratings (Fig 1C). Using this modeling approach allowed us to characterize the absolute distance between the ratings along with the subjects' confidence ratings in a single measurement of trial-specific choice discriminability. Importantly, high entropy corresponds to lower choice discriminability that is induced by similar ratings. To estimate the requisite softmax (sensitivity or precision) parameter, we modeled performance in terms of entropy (H) over trials (and subjects) using a simple linear regression model. The ensuing behavioral model provided an estimate of the precision parameter (β) and associated measure of trial-specific choice discriminability for each subject.

In detail, we want to score the difficulty of each trial. This difficulty is the entropy (H) of the choice probability (p), based upon a softmax function of the log odds ratio of a target (stranger) preference (T) being sampled from the distributions of (nonanchor) reference subjects A and B. Let the preference of individual i have a mean μ_i and standard deviation σ_i, then the log probability of sampling T from the preference distribution of the i-th reference subject is (ignoring constants)

$$L_i = -\frac{1}{2}\frac{(T-\mu_i)^2}{\sigma_i^2}. \quad (1)$$

If we assume a precision of β, then the probability of choosing subject A over B is a softmax function of the log odds ratio:

$$P_A = \frac{\exp(\beta \cdot L_A)}{\sum_{i\subset\{A,B\}}\exp(\beta \cdot L_i)} \quad (2)$$

and the difficulty is the entropy:

$$H = \sum_{i\subset\{A,B\}} - P_i ln P_i. \quad (3)$$

This will give difficulties between 0 and ln(2), i.e., 0.6931. Given the mean and standard deviation reported by subjects, we can evaluate the probability of choosing each (nonanchor) individual on each trial, given the stranger's target preference. We used the Bayesian information criterion (BIC) [24] to determine if a signal detection model including subjective confidence ratings—as the standard deviation—outperforms a distance-only model. Notably, we found that the model including confidence ratings (BIC = −39,056) outperformed a simpler distance-only model (BIC = −38,387), for which the lower BIC signifies the greater model evidence. In short, this provides strong evidence for a model based on confidence ratings.

This model of choice behavior provided trial-specific measures of choice uncertainty (H) that enabled us to identify its fMRI correlates. Following previous work [25–27], we used the mean precision parameter (β), evaluated over subjects to compute trial-specific choice entropies as a predictor for our fMRI responses. We found that choice entropy negatively correlated with performance over trials ($t = -10.9$; $P < 0.001$). As might be expected, we observed a significant effect of condition for mean choice entropy ($F[2,22] = 17.6$; $P < 0.001$; see Fig 2F), for which choice entropy was significantly higher for self than canonical ($t[23] = 6.06$; $P < 0.001$) or friend ($t[23] = 4.23$; $P < 0.001$) anchor trials (Fig 2F). This was likely due to lower confidence (i.e., memory demands) for friend and canonical ratings, relative to ratings of self preferences, as well as the smaller mean absolute distances in self anchor trials in relation to canonical anchor trials.

fMRI analyses

Choice discrimination. To test how strangers' preferences are compared to personally known people, we characterized the brain's response to uncertainty in preference discrimination. Specifically, we were interested in what brain regions related to choice discrimination in different absolute reference frames.

In a whole-brain analysis—comparing differences in entropy effects between the three conditions (self, friend, and canonical)—the only significant entropy-by-condition interaction and the strongest effect of any area in the brain for this contrast was in a right entorhinal/subicular area (x = 24, y = −28, z = −22; F-stat: 9.87; Z-score = 3.46; SVC peak-voxel $P = 0.034$; Fig

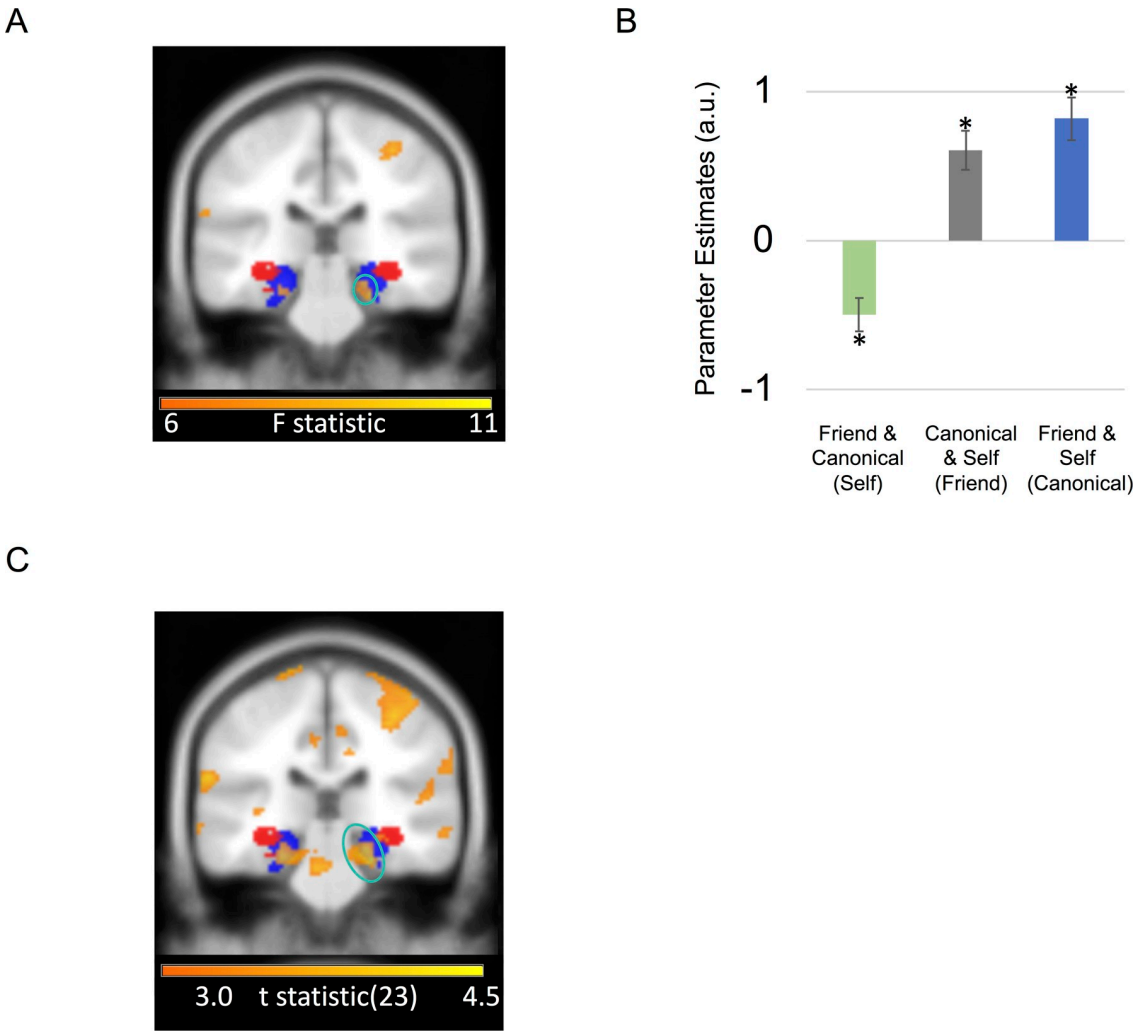

Fig 3. Entorhinal/Subicular choice discrimination effects. A. Coronal image of right entorhinal/subicular region exhibiting an effect of choice discriminability/entropy by condition circled in turquoise. B. Effect size for a 10-mm sphere around right entorhinal/subicular region exhibiting effect of choice entropy by condition (mean ± SEM). Asterisk marks significance at $P < 0.05$. See S2 Data for subject data. C. Coronal image showing right entorhinal/subicular (circled in turquoise) correlation with choice entropy for friend and canonical anchor trials (i.e., choices involving self-comparisons) versus self anchor trials (i.e., trials comparing canonical versus friend ratings). Portion of left entorhinal/subicular region showing same effect is also visible. A positive effect size indicates a positive BOLD correlation with choice entropy (i.e., ambiguous choices), whereas a negative effect size indicates a negative BOLD correlation with choice entropy in the same comparison (i.e., straightforward choices). All highlighted regions survived FWE correction for multiple comparisons at $P < 0.05$ and are displayed at an uncorrected statistical threshold of $P < 0.005$ for display purposes. For visualization purposes, entorhinal/subicular (blue) and hippocampal body (red) probabilistic masks from the Jülich SPM Anatomy toolbox are presented [28]. BOLD, blood oxygen level-dependent; FWE, family-wise error; SPM, statistical parametric mapping.

https://doi.org/10.1371/journal.pbio.3000230.g003

3A and 3B), extending into anterior parahippocampal cortex. In other words, the right entorhinal/subicular effect of discriminability depended upon the anchor condition.

Subsequent *t* tests on the entorhinal/subicular region exhibiting choice discriminability/entropy effects indicated that there was a significant positive correlation with entropy (i.e., less discriminable/ambiguous choices) for canonical (t[23] = 2.75; $P = 0.011$) and friend (t[23] = 2.36; $P = 0.027$) anchor trials, while there was a significant negative correlation with entropy (i.e., more discriminable/straightforward choices) for self anchor trials (t[23] = −2.39; $P = 0.025$; Fig 3B). Contrasting canonical and friend versus self anchor trials, we observed that

the right entorhinal/subicular effect (right: Z-score = 4.02; peak voxel $P = 0.004$; Fig 3C) was the strongest effect of any area in the brain for this contrast. Note that canonical and friend anchor trials involved choices with self preferences. Subjects either decided whether a stranger's rating for a scenario was closer to the self versus canonical individual (friend anchor) or the self versus the friend (canonical anchor). Conversely, self anchor trials involved deciding whether a stranger's rating was closer to the friend versus the canonical individual. In other words, the entorhinal/subicular region responded to more fine-grained/ambiguous choices involving self-comparisons but readily discriminable choices otherwise. However, it is important to note that our model did not predict a significant negative correlation with entropy for the self anchor condition, only that this condition was typically more demanding for subjects, so the negative direction of this effect should be interpreted with caution.

We then investigated which brain regions responded to choice entropy (i.e., how discriminable the choices were). However, we did not find any significant regions responding to increasing (i.e., a positive correlation between the fMRI signal and choice entropy/less discriminable choices) or decreasing choice entropy (i.e., a negative correlation between the fMRI signal and choice entropy/more discriminable choices) anywhere in the brain.

Anchor rescaling. In our task, reference frame transformations rely on flexibly relating different known individuals' ratings to each other. We wanted to capture the initial demands of mentally rescaling the anchor and, consequently, the corresponding stranger from its observed (relative) position on the screen to its actual rating (absolute position) on the scale. To test this, we investigated which regions responded to how far the anchor's preference deviated from the middle of the scale (Anchor Rescaling |anchor rating -5|). In a whole-brain analysis, the only significant main effect of increased anchor rescaling toward the limits of the scale was in the superior parietal lobule (SPL) bilaterally (left: x = −57, y = −52, z = 44; Z-score = 4.09; family-wise error [FWE] cluster $P = 0.024$; right: x = 33, y = −64, z = 54; Z-score = 3.99; FWE cluster $P = 0.005$; S3 Fig).

However, we did not observe any significant effects for decreased anchor rescaling (maintaining the rating in the middle of the scale). Likewise, we did not observe any regions showing an interaction with anchor condition.

Accuracy. Further characterizing the functional contribution of different brain regions, we asked if regional responses during memory-guided decisions depended on whether subjects made a correct or incorrect choice for each trial. In a whole-brain analysis, we observed significant activation for correct trials in the right ventral striatum (x = 24, y = 8, z = −6; Z-score = 4.69; FWE cluster $P < 0.001$; Fig 4A and 4B) extending into white matter and left posterior parietal cortex (PPC) in the depth of intraparietal sulcus (x = −24,y = −64, z = 42; Z-score = 4.30; FWE cluster $P = 0.005$; S4 Fig). We did not observe any significant activation that preceded incorrect choices, nor significant interactions between anchor condition and accuracy.

Finally, to test whether the right ventral striatum accuracy effect was driven by choices for which highest/lowest judgments between the two choice individuals needed to be made, we split decision-making trials in terms of whether a choice required determining which choice option was highest/lowest instead of closest. Ignoring the three anchor conditions, we split the data into two conditions: one for which the stranger was between the two choice individuals and the second for which the stranger was either higher or lower than both choice individuals. We asked whether subjects who performed better for the latter scenario also recruited the ventral striatum when making highest/lowest versus proximity judgments. We found a between-subject correlation between our right ventral striatal effect for highest/lowest judgments and subject performance for highest/lowest versus proximity judgments (r = 0.561; $P = 0.004$) (Fig 4C).

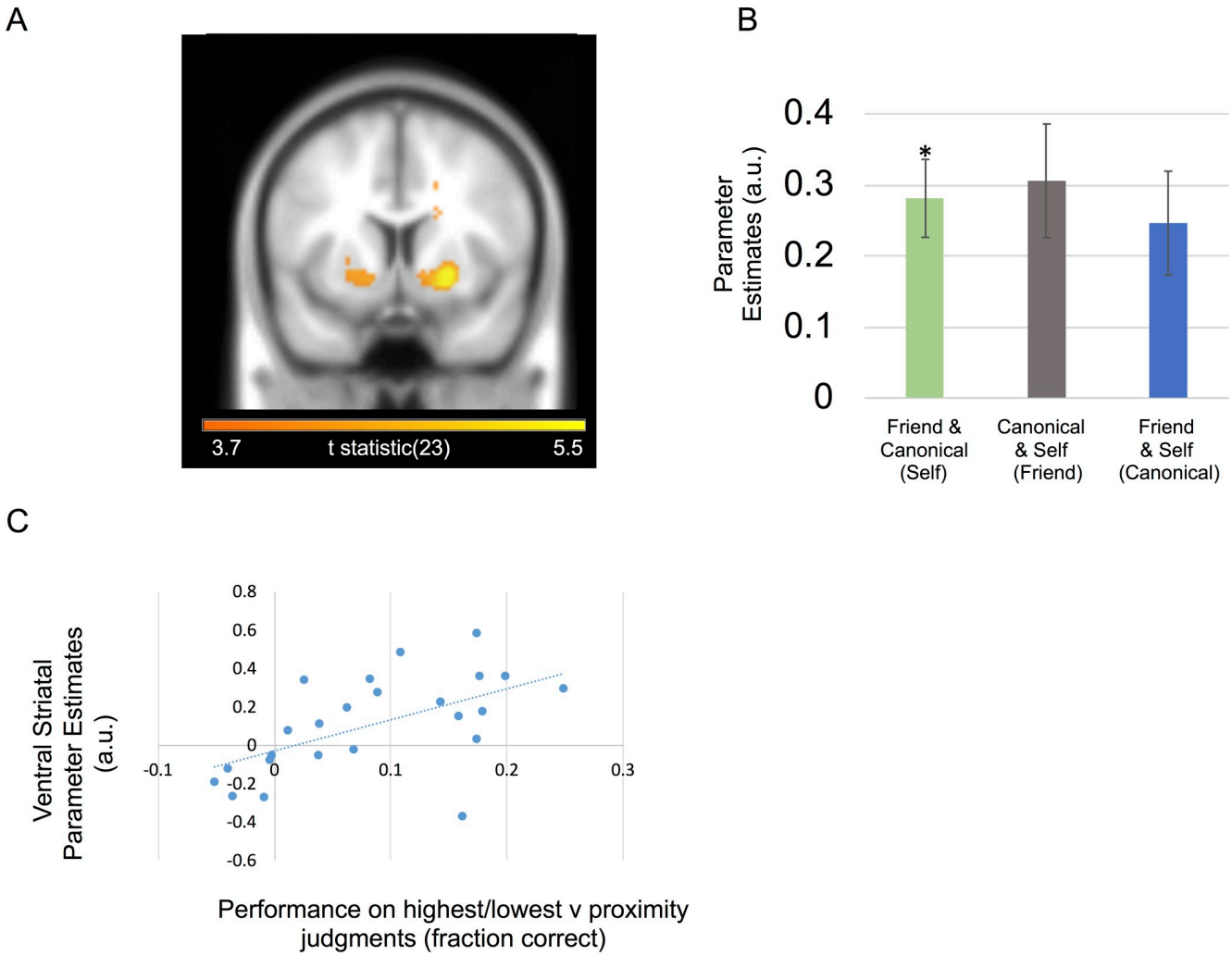

Fig 4. Striatum and decision accuracy. A. Ventral striatal activity related to correct versus incorrect choices. The ventral striatal cluster survived cluster-level FWE correction at $P < 0.05$ and is displayed at an uncorrected statistical threshold of $P < 0.001$. B. Effect sizes for a 10-mm sphere around right ventral striatum peak voxel (mean ± SEM). Individuals being compared listed below with anchor in parentheses. A positive effect size indicates a positive BOLD correlation with correct choices. Asterisk marks significance at $P < 0.05$. C. Plot showing between-subject correlation for subjects' ventral striatal fMRI signals with behavioral performance. Ventral striatal effects were for highest/lowest judgments versus proximity judgment trials (GLM2). Behavioral performance was taken from subjects' performance on trials, where highest/lowest judgments could be used, versus their performance on trials where a proximity judgment could be used. Subjects who performed better for highest/lowest judgments exhibited increased ventral striatal activity for the same contrast. See S3 Data for subject data from B and C. BOLD, blood oxygen level-dependent; fMRI, functional magnetic resonance imaging; GLM, general linear model.

https://doi.org/10.1371/journal.pbio.3000230.g004

Remaining fMRI analyses. Asking whether the time spent deliberating and trying to remember a particular choice option's preferences influenced any neural responses during our task, we investigated whether any fMRI signals during the social decision-making task correlated with RT. We observed signals in the PPC/precuneus (left: x = −18, y = −58, z = 44; Z-score = 4.49; FWE cluster $P < 0.001$; right: x = 30, y = −73, z = 42; Z-score = 4.07; FWE cluster $P = 0.001$; S5 Fig), left motor cortex (x = −33, y = 5, z = 48; Z-score = 4.35; FWE cluster $P = 0.033$), and lateral occipital cortex (left: x = −24, y = −97,z = −6; Z-score = 4.26; FWE cluster $P < 0.001$; right: x = 27, y = −91, z = 4; Z-score = 4.35; FWE cluster $P = 0.033$) that positively correlated with RT. However, we observed no significant negative correlation with RT anywhere in the brain nor significant interactions between anchor condition and RT. Lastly,

we also tested whether there were neural responses specifically linked to participants' subjective confidence ratings for a given choice and did not observe significant responses in any brain region.

Discussion

Using computational modeling, fMRI, and a novel memory-guided decision-making paradigm, we asked how different brain regions integrate relatively coded knowledge of different people's personal attributes within absolutely coded metric spaces (Fig 1). Focusing on reference frame-sensitive responses, we identified an entorhinal/subicular region that related to the absolute distance between the stranger's rating and the ratings of choice options differently depending on whether a self-comparison was involved (Fig 3). In parallel, SPL activity increased when the anchor required a mental shift from the middle of the scale toward the periphery (S3 Fig). Finally, we found that striatal responses also preceded correct choices, which were partially driven by decisions about which individual had the highest or lowest preference rating (Fig 4). In what follows, we relate these findings to the wider literature—and to the entorhinal/subicular responses we observed. We then speculate on potential neural computations induced by our task.

Entorhinal/subicular representations of social knowledge along multiple scales

We observed entorhinal/subicular responses to more precise, fine-grained choices if self-comparisons were involved but more straightforward choices otherwise. This result is partially a consequence of lower confidence when rating the friend and canonical individual as well as smaller mean absolute distances between those two individuals and the stranger, which induced significantly higher choice entropy for the self anchor condition, i.e., a more ambiguous/less discriminable choice scenario. Still, significantly higher choice entropy for the self anchor condition doesn't imply that there should be a negative correlation between the entorhinal/subicular fMRI signal and entropy for the self anchor condition. It only hints that the correlation is likely to be lower than the canonical and friend anchor conditions. Therefore, we can't make any definitive conclusions about the direction of the effects in the entorhinal/subicular entropy-by-condition interaction beyond the entorhinal/subicular region's sensitivity to anchor conditions with self-comparisons. Crucially, despite the difference between the anchor conditions in mean choice entropy, a similar distinction was not observed in the hippocampal body or other brain regions. Notably, in rodents, hippocampal place representations are modulated by self-location and are continuous [29]. In contrast, entorhinal/subicular grid as well as object and boundary vector representations use multiple reference frames and can either be continuously or discretely coded [18,30–31]. This highlights a potential functional dissociation to memory-guided decision-making involving different points of reference, for which the body of the hippocampus could relate to self-referenced sampling of prior experience [32–35]. While in contrast, we observe entorhinal/subicular sensitivity to the depth of personal knowledge for different familiar individuals (i.e., how well we know someone's personal preferences). Further support for this distinction stems from the putative role of the entorhinal cortex [29,36–37] and subicular region [38] in integrating incoming sensory input with learned hippocampal representations. Building on recent studies of macaque and human entorhinal cortex in spatial and nonspatial tasks, our results potentially speak to the organizational principles governing metrically coded maps [20,39–45] along with the implicit encoding of discrete graphs [21], which may be located within the same brain region. This architecture

portends a domain general role for entorhinal cortex in memory-guided decision-making involving multiple reference frames.

Parietal rescaling of metrically coded preferences

In our task, participants retrieve and nonlinearly rescale different mental number lines of personal preferences. Following previous observations of posterior parietal involvement in maintaining a mental number line [46–47] and manipulating the position of items in spatial working memory [48], we observe bilateral SPL responses during trials when participants need to mentally rescale the anchor's relative position in the center toward an absolute position on the periphery of the scale. Moreover, our observation of SPL involvement in mental rescaling of metrically scaled preferences meshes well with the putative notion that parietal areas track magnitudes [49].

Striatal involvement in knowledge-guided social decision-making

We observed a ventral striatal signal corresponding to correct choices, which also related to choices for which highest/lowest—as opposed to proximity—judgments could be made. This distinction between hippocampal–entorhinal versus striatal responses to different knowledge-guided decision-making strategies closely follows spatial navigation strategies for which the subjects align themselves to a single landmark instead of a boundary in order to infer the direction of a goal location [50]. The implicit functional neuroanatomy may parallel the dissociation between hippocampal and striatal responses observed in the current study. This follows since boundary-oriented navigation is linked to the hippocampus, whereas landmark-based navigation is related to the striatum [51]. More generally, this striatal versus hippocampal dissociation highlights a potential mechanism for how reinforcement/procedural learning could reduce metrically coded relational knowledge into more efficiently usable heuristics [52–53], paralleling categorical versus coordinate-based judgments in spatial cognition [54–55].

Allocentricity and the dimensionality of preferences

Our findings highlight the role of the hippocampal formation, namely the entorhinal cortex and subiculum, in the functional anatomy of how we transform relative and absolute reference frames during decision-making. However, since all of our conditions involve a transformation, it is unclear whether humans ever preferentially use an absolute or "allocentric" frame of reference during decision-making without drawing upon their own frame of reference. Even in spatial and episodic memory, this question is difficult to resolve (see [56]) since self-referencing helps us relate past experience to our current environment [57]. Notably, even rodent hippocampal place cells, the building block of the cognitive map, can be distorted by local egocentric cues (see [58] for an example). Useful clues about how we flexibly transform relative and absolute reference frames come from the social psychology literature. A subset of social psychology has focused on how individualized representations of others' preferences are generated by anchoring to a known preference and then adjusting accordingly, a phenomenon known as "anchoring and adjustment" [59–61]. Given their similarities, jointly studying "anchoring and adjustment" with boundary-oriented navigation may offer a promising avenue for translational research across species and levels of analysis.

We tested metrically coded preferences along a single dimension (namely the likelihood of people preferring things), but the true dimensionality of personal preferences is less clear. It is plausible that we learn about others' preferences within a multidimensional trait space [62]. Yet we do not know the number of dimensions that support this trait space [63–64]. Further

work may help relate what we know about navigating physical space with the mental exploration of more abstract spaces [22,65].

Our study induces a spatial (metric) strategy, preventing us from asking whether humans must use map-like coding in order to relate others' preferences to their own. Furthermore, decisions in our task involve an abstract one-dimensional spatial discrimination, in which subjects determine the relative proximity of a stranger's rating to the nonanchor individuals. Future work can implicitly test discrimination of metrically coded decision variables in absolute reference frames more implicitly (i.e., without an explicit spatial element) to determine whether the spatial element is required for hippocampal–entorhinal involvement. Still, theoretical work has provided support for the use of a spatial strategy, for which nonhuman primate research has investigated social cognition in terms of coordinate transforms [66]. Social coordinate transformation experiments have captured how social variables are encoded in individual neurons—and how encoding changes over different computational stages during social decision-making [67] like current versus long-term frames of reference [68]. Extending such work to abstract knowledge may potentially help us understand how coordinate transformations can generally guide everyday decisions.

Conclusion

Metric coding of decision variables informs decisions by providing coordinates and boundaries that can be translated between different frames of reference. We provide evidence that neural computations—that integrate relative and absolute coordinates during spatial navigation—also extend to relating others' personal attributes to our own. Consequently, these data provide important clues about how hippocampal–entorhinal map-like coding may facilitate memory-guided decision-making in a domain general manner.

Materials and methods

Ethics statement

Subjects were studied and compensated and gave informed written consent to participate. This study was approved by the local research ethics committee at University College London (approval reference: 1825/003). The study was conducted in accordance with Declaration of Helsinki protocols.

Subjects

Twenty-four healthy adult subjects (16 female; mean age of 25.5 y; SD of 5.38 y) took part in the experiment. All subjects were right-handed, had normal or corrected-to-normal vision, and reported good health with no prior history of neurological disease.

Task

Stimuli were presented using the Cogent (http://www.vislab.ucl.ac.uk/cogent.php) toolbox running in MATLAB (Mathworks, Natick, MA, United States). Subjects performed a self-paced (max 9 s), forced-choice, social decision-making task featuring 100 different personal preferences for 3 personally familiar individuals, which included themselves. Subjects viewed a personal preference for a novel stranger, represented by an avatar (Fig 1), that was presented on a scale relative to 1 of 3 known individuals (anchor). Immediately prior to scanning, subjects were first trained to infer the stranger's rating and then look below the scale in order to decide which of the 2 remaining familiar individuals was closer to that rating. All of

the information needed to perform the task was presented at once on the screen, and the only aspects of the task that varied from trial to trial were the anchor and choice options.

All ratings were obtained from subjects approximately 45 minutes prior to fMRI scanning. Subjects gave likelihood ratings about 110 everyday scenarios (e.g., eating spicy food; see S1 Table for all scenarios) from 1–9 on a 0–10 scale (0 being impossible to 10 being extremely likely) for themselves and two other familiar individuals. For one of the familiar individuals (friend), subjects were asked to choose their closest friend of the same gender that had the most distinct personality from the subject and—unlike the subject—ideally lived outside of London, in order to induce different ratings between individuals. The third individual was a typical/canonical individual of the same gender named Mr./Ms. Normal. Mr./Ms. Normal was supposed to correspond with what they thought a normal person/exemplar at their stage of life would do for each scenario (Fig 1A). During the rating period, subjects were instructed to keep track of how their ratings related to each other for a given scenario (e.g., the participant being a bit more likely to have spicy food than their friend). Crucially, subjects also gave confidence ratings for the canonical exemplar and their friend on every scenario on a scale from 1–5 (No Idea to Very Sure) in order to assess the consistency of their rating (Fig 1A). As a second confirmation of rating consistency, subjects also rated the familiar individuals for every scenario after the fMRI task.

Subjects then performed a brief practice version of the fMRI social decision-making task outside of the scanner, for which subjects viewed a personal preference for a stranger that was presented on a 0–10 scale relative to one of the known individuals (anchor). Subjects had a maximum of 9 seconds to decide whether the stranger's rating was closer to the 2 remaining (nonanchor) individuals. The anchor was indicated by presenting their initials, which would either be the friend's initials, ME (Self), or MN, which was an abbreviation for Mr./Ms. Normal (Canonical). All information related to the decision was presented at once, with the scenario being listed above the stranger and anchor individual on the scale (Fig 1B). Directly below the scale "closer to self/friend/canonical individual (A) or self/friend/canonical individual (B)" was written. After making a decision, there was then a jittered ITI period (mean = 2.43 s; range = 0.25–9 s) for which a white fixation point overlaid on a black background was presented.

Crucially, the anchor individual was always placed in the middle of the scale so that subjects needed to use prior social knowledge in order to infer the stranger's absolute preference and form a mental number line of the nonanchor preferences. In other words, subjects had to infer the stranger's true (absolute) position in relation to the anchor's rating for that scenario and the closest boundary (0 or 10). For example, if the stranger was three-fourths to the right of an anchor individual that was rated a 9, the participant would infer that the stranger's rating was three-fourths of the way between 9 and 10 (the right boundary of the scale). Consequently, the subject would indicate the stranger's rating would approximately be near 10 (actual rating = 9.75). We assumed that subjects represented people's preferences on this number line, similar to a mental number line [46], thereby enabling them to choose the individual (A or B) that was closest to the stranger. If both individuals in the choice were the same or equidistant from the stranger, subjects were instructed that either answer was counted as correct. Same or equidistant trials were not used in either behavioral or fMRI analyses.

Subjects then practiced the task using the last 10 scenarios they rated, which were repeated 3 times each. On the first few practice trials, subjects verbally rehearsed transforming the anchor's rating from the middle of the screen to its actual (absolute) position and then inferring the stranger's rating with verbal feedback from the experimenter until they performed the transformation correctly.

Then, during fMRI scanning, subjects performed the task for the remaining 100 scenarios in 3 different self-paced runs (once for each anchor individual), each lasting approximately 10 minutes (a maximum of 15 minutes). From a relative viewpoint, the stranger was either ± one-fourth or three-fourths of the way between the anchor individual and the boundary ratings of 0 and 10, which was presented equally by run and condition. Subjects were instructed that it was a different stranger on each trial, so the stranger didn't conserve any preferences. To further emphasize the lack of conserved preferences, the stranger avatar randomly alternated between five colors (red, green, yellow, magenta, and cyan). Once again after completing the fMRI task, subjects gave likelihood ratings for the friend and canonical individuals outside of the scanner.

Computational model

We used a trial-by-trial computational model of subjects' performance in order to quantify how subjects' individual ratings and confidence judgments determined subjects' choice discriminability during social decision-making (see Fig 1C). Choice discriminability (or inverse precision) was measured using Shannon entropy [69]. Shannon entropy (H) was calculated by estimating the distribution of choice probabilities using a softmax function of individual ratings. This included the standard deviation (σ_i) derived from subject's confidence ratings (C_i) for each scenario ($\sigma_i = 1$ for all self ratings), in which the constant term accommodated the assumed stability (reduced memory demands) of self ratings as well as the dynamic range of confidence ratings.

$$\sigma_i = 1 + \frac{1}{2}(5 - C_i) : \; C_i \sqsubset \{1, , 5\} \tag{4}$$

Furthermore, the inverse temperature parameter (β) of the softmax function was optimized using each subject's trial-by-trial performance. We constructed predictions of neuronal responses in terms of the Shannon entropy (H) of the choice probability in each trial for fMRI [70].

We optimized subject-specific parameters across trials using maximum likelihood estimation and the optimization toolbox in MATLAB (MathWorks, Inc). We then calculated trial-by-trial parameter estimates of H (choice discriminability) using the group average softmax (precision or inverse temperature) parameter. The ensuing trial-by-trial choice entropy measures were then used to predict BOLD responses in our neuroimaging analyses.

fMRI acquisition

Functional images were acquired on a 3T Siemens Trio scanner. BOLD T2*-weighted functional images were acquired using a gradient-echo EPI pulse sequence acquired obliquely at 45˚ with the following parameters: repetition time, 3,360 ms; echo time, 30 ms; slice thickness, 2 mm; interslice gap, 1 mm; in-plane resolution, 3 × 3 mm; field of view, 64 × 72 mm^2; 48 slices per volume. A field map using a double-echo FLASH sequence was recorded for distortion correction of the acquired EPI [71]. After the functional scans, a T1-weighted 3D MDEFT structural image (1 mm^3) was acquired to coregister and display the functional data [70].

fMRI analysis

Functional images were processed and analyzed using SPM12 (www.fil.ion.ucl.uk/spm). The first 5 volumes were discarded to allow for T1 equilibration. Standard preprocessing included bias correction for within-volume signal intensity differences, correction for differences in slice acquisition timing, realignment/unwarping to correct for interscan movement, and

normalization of the images to an EPI template (specific to our sequence and scanner) that was aligned to the T1 Montreal Neurological Institute (MNI) template [70]. Finally, the normalized functional images were spatially smoothed with an isotropic 8-mm full-width half-maximum Gaussian kernel. For the model described below, all regressors, with the exception of 6 movement parameters of no interest, were convolved with the SPM hemodynamic response function. Data were also high-pass filtered (cut-off period = 128 s). Statistical analyses were performed using a univariate GLM with an event-related experimental design [70].

GLM1. There were 2 periods of interest: the self-paced (9-s maximum) social decision-making and jittered baseline ITI, which were modeled as boxcar functions and convolved with a canonical hemodynamic response function (HRF) to create regressors of interest. For each social decision-making regressor (self, friend, and canonical anchor trials), there were parametric regressors based on accuracy (whether the choice was correctly answered; 1 = incorrect choice; 2 = correct choice), anchor rescaling, choice entropy (discriminability), RT, and subjective confidence ratings. Inferences about these effects were based upon *t* and F tests using the standard summary statistic approach for second-level random effects analysis.

GLM2. In a follow-up analysis to assay whether the ventral striatum accuracy effect was driven by choices for which a highest or lowest judgment between the 2 choice individuals needed to be made, we split decision-making trials in terms of whether a choice required determining which choice option was highest/lowest instead of closest. Ignoring the 3 conditions, we split the data into 2 conditions: one for which the target was between the 2 choice individuals and the second for which the target was either higher or lower than both choice individuals.

All initial analyses were whole-brain analyses. Subsequently, posthoc statistical analyses were conducted using 10-mm radius spheres in MarsBar toolbox [72] within SPM12 around the respective peak-voxel specified in the GLM analysis. This allowed us to compare the effects of different parametric regressors of interest (e.g., to determine whether an accuracy effect was present in a region defined by an orthogonal main effect of choice discriminability). This ensured we did not make any biased inferences in our posthoc analyses. We used 10-mm radius spheres for posthoc statistical analyses—instead of clusters—since our entorhinal/subicular effects were corrected for multiple comparisons at the peak-voxel level.

Given the previously hypothesized role of the entorhinal/subicular region and hippocampus in absolute versus relative coding of environmental cues, we report whether peak-voxels in these regions survive small-volume correction for multiple comparisons ($P < 0.05$) based on bilateral ROIs in the entorhinal/subicular region (mask used in [20–21]) and the hippocampus (mask created using Neurosynth [73]). For all analyses outside of the ROIs, we report activations surviving an uncorrected statistical threshold of $P = 0.001$ and correction for multiple comparisons at the whole-brain level (FWE $P < 0.05$). Coordinates of brain regions are reported in MNI space.

Supporting information

S1 Fig. Ratings overlap. Significant effect of condition for ratings overlap (the same ratings) between the two individuals ($P < 0.001$). Individuals being compared are listed below each bar with the corresponding anchor/condition name listed in parentheses. Occurrences are out of the 100 trials per condition. See S4 Data for subject data.
(PDF)

S2 Fig. Absolute distances and reaction time. Significant relationship ($P < 0.001$) between decision speed (reaction time) and the absolute distance between strangers' ratings and the nonanchor individuals for each trial. The absolute value of absolute distances were rounded to

the closest integer and plotted from 1 to 8. Seven and 8 on the x-axis are shaded in gray, because only 18/24 and 13/24 subjects had trials with absolute distances of 7 and 8, respectively. Error bars showing mean ± SEM. See S5 Data for subject data.
(PDF)

S3 Fig. Superior parietal lobe rescaling effect. Sagittal image showing superior parietal lobule effect of mentally rescaling anchor towards the periphery in either direction, as seen in Fig 1D. Highlighted region survived cluster-level FWE correction at $P < 0.05$ and image is displayed at an uncorrected statistical threshold of $P < 0.001$. FWE, family-wise error
(PDF)

S4 Fig. Parietal accuracy effect. Coronal image of increased intraparietal sulcus activity for correct versus incorrect choices. Highlighted region survived cluster-level FWE correction at $P < 0.05$ and image is displayed at an uncorrected statistical threshold of $P < 0.001$. FWE, family-wise error.
(PDF)

S5 Fig. Reaction time effects. Images of increased posterior parietal cortex and precuneus activity for slower RTs. Highlighted region survived cluster-level FWE correction at $P < 0.05$ and image is displayed at an uncorrected statistical threshold of $P < 0.001$. RT, reaction time.
(PDF)

S1 Table. List of Rated Scenarios. Last 10 were used during practice trials and first 100 were used for the fMRI task. fMRI, functional magnetic resonance imaging.
(DOCX)

S1 Data. Data underlying plots in Fig 2.
(XLSX)

S2 Data. Data underlying plots in Fig 3B.
(XLSX)

S3 Data. Data underlying plots in Fig 4B and 4C.
(XLSX)

S4 Data. Data underlying plot in S1 Fig.
(XLSX)

S5 Data. Data underlying plot in S2 Fig.
(XLSX)

Acknowledgments

The authors would like to thank Asaf Gilboa, Jochen Michely, Philipp Schwartenbeck, and Geert-Jan Will for helpful discussion along with Martin Chadwick and Mona Garvert for providing an entorhinal/subicular mask. We thank Jacob Bellmund and Joshua Julian for helpful comments on a previous version of this manuscript. The authors would also like to thank Megan Creasey and Clive Negus for help with scanning and the Wellcome Centre for Human Neuroimaging for providing facilities.

Author Contributions

Conceptualization: Raphael Kaplan.

Data curation: Raphael Kaplan.

Formal analysis: Raphael Kaplan.

Funding acquisition: Raphael Kaplan.

Investigation: Raphael Kaplan.

Methodology: Raphael Kaplan, Karl J. Friston.

Project administration: Raphael Kaplan.

Supervision: Karl J. Friston.

Writing – original draft: Raphael Kaplan.

Writing – review & editing: Raphael Kaplan, Karl J. Friston.

References

1. Eichenbaum H. The Hippocampus as a Cognitive Map . . . of Social Space. Neuron. 2015; 87:9–11. https://doi.org/10.1016/j.neuron.2015.06.013 PMID: 26139366
2. Kumaran D, Maguire EA The Human Hippocampus: Cognitive Maps or Relational Memory? J Neurosci. 2005; 25:7254–59. https://doi.org/10.1523/JNEUROSCI.1103-05.2005 PMID: 16079407
3. Kumaran D, Melo HL, Duzel E. The emergence and representation of knowledge about social and non-social hierarchies. Neuron. 2012; 134, 653–8.
4. Kumaran D, Banino A, Blundell C, Hassabis D, Dayan P. Computations Underlying Social Hierarchy Learning: Distinct Neural Mechanisms for Updating and Representing Self-Relevant Information. Neuron. 2016; 92, 1135–47. https://doi.org/10.1016/j.neuron.2016.10.052 PMID: 27930904
5. Schiller D, Eichenbaum H, Buffalo EA, Davachi L, Foster DJ, Leutgeb S, Ranganath C. Memory and Space: Towards an Understanding of the Cognitive Map. J Neurosci. 2015; 35:13904–11. https://doi.org/10.1523/JNEUROSCI.2618-15.2015 PMID: 26468191
6. Zeithamova D, Maddox WT, Schnyer DM. Dissociable prototype learning systems: evidence from brain imaging and behavior. J Neurosci. 2008; 28:13194–201. https://doi.org/10.1523/JNEUROSCI.2915-08.2008 PMID: 19052210
7. Mack ML, Love BC, Preston AR Dynamic updating of hippocampal object representations reflects new conceptual knowledge. Proc Natl Acad Sci USA. 2016; 113:13203–13208. https://doi.org/10.1073/pnas.1614048113 PMID: 27803320
8. Mack ML, Love BC, Preston AR Building concepts one episode at a time: The hippocampus and concept formation. Neurosci Lett. 2018; 680:31–38. https://doi.org/10.1016/j.neulet.2017.07.061 PMID: 28801273
9. McNaughton BL, Battaglia FP, Jensen O, Moser EI, Moser MB. Path integration and the neural basis of the 'cognitive map'. Nat Rev Neurosci. 2006; 7:663–78. https://doi.org/10.1038/nrn1932 PMID: 16858394
10. Hafting T, Fyhn M, Molden S, Moser MB, Moser EI. Microstructure of a spatial map in the entorhinal cortex. Nature. 2005; 436:801–6. https://doi.org/10.1038/nature03721 PMID: 15965463
11. Boccara CN, Sargolini F, Thoresen VH, Solstad T, Witter MP, Moser EI, Moser MB. Grid cells in pre- and parasubiculum. Nat Neurosci. 2010; 13:987–94. https://doi.org/10.1038/nn.2602 PMID: 20657591
12. O'Keefe J, Dostrovsky J. The hippocampus as a spatial map: Preliminary evidence from unit activity in the freely-moving rat. Brain Res. 1971: 34:171–5. PMID: 5124915
13. O'Keefe J, Burgess N. Geometric determinants of the place fields of hippocampal neurons. Nature. 1996; 381:425–28. https://doi.org/10.1038/381425a0 PMID: 8632799
14. Burgess N, Jackson A, Hartley T, O'Keefe J. Predictions derived from modelling the hippocampal role in navigation. Biological cybernetics. 2000; 83:301–12. https://doi.org/10.1007/s004220000172 PMID: 11007303
15. Hartley T, Burgess N, Lever C, Cacucci F, O'Keefe J. Modeling place fields in terms of the cortical inputs to the hippocampus. Hippocampus. 2000; 10:369–79 https://doi.org/10.1002/1098-1063(2000)10:4<369::AID-HIPO3>3.0.CO;2-0 PMID: 10985276
16. Taube JS, Muller RU, Ranck JB. Head-Direction Cells Recorded from the Postsubiculum in Freely Moving Rats. I. Description and Quantitative Analysis. J Neurosci. 1990; 10:420–35. PMID: 2303851
17. O'Keefe J, Nadel L. The Hippocampus as a Cognitive Map. 1978:114–52 (Oxford Univ Press)

18. Hartley T, Lever C, Burgess N, O'Keefe J. Space in the brain: how the hippocampal formation supports spatial cognition. Philos Trans R Soc Lond B. 2013; 369:20120510.
19. Howard LR, Javadi AH, Yu Y, Mill RD, Morrison LC, Knight R, Loftus MM, Staskute L, Spiers HJ. The hippocampus and entorhinal cortex encode the path and Euclidean distances to goals during navigation. Curr Bio. 2014; 24:1331–40.
20. Chadwick MJ, Jolly AE, Amos DP, Hassabis D, Spiers HJ. A goal direction signal in the human entorhinal/subicular region. Curr Biol. 2015; 25:87–92. https://doi.org/10.1016/j.cub.2014.11.001 PMID: 25532898
21. Garvert MM, Dolan RJ, Behrens TE A map of abstract relational knowledge in the human hippocampal-entorhinal cortex. Elife. 2017; 6.
22. Kaplan R, Schuck NW, Doeller CF. The Role of Mental Maps in Decision-Making. Trends Neurosci. 2017; 40:256–9 https://doi.org/10.1016/j.tins.2017.03.002 PMID: 28365032
23. Tanner WP Jr, Swets JA. A decision-making theory of visual detection. Psychological Review, 1954; 61:401–9. PMID: 13215690
24. Schwarz G. Estimating the dimension of a model. Ann Stat.1978; 6:461–64.
25. Daw ND, O'Doherty JP, Dayan P, Seymour B, Dolan RJ. Cortical substrates for exploratory decisions in humans. Nature. 2006; 441:876–9. https://doi.org/10.1038/nature04766 PMID: 16778890
26. Glascher J, Daw N, Dayan P, O'Doherty JP. States versus rewards: dissociable neural prediction error signals underlying model-based and model-free reinforcement learning. Neuron. 2010; 66:585–95. https://doi.org/10.1016/j.neuron.2010.04.016 PMID: 20510862
27. Daw ND. in Decision Making, Affect, and Learning: Attention and Performance XXIII, eds:Delgado M. R., Phelps E.A., Robbins T.W. (Oxford Univ Press, Oxford) (2011).
28. Amunts K, Kedo O, Kindler M, Pieperhoff P, Mohlberg H, Shah NJ, Habel U, Schneider F, Zilles K. Cytoarchitectonic mapping of the human amygdala, hippocampal region and entorhinal cortex: intersubject variability and probability maps. Anat Embryol (Berl). 2005; 210:343–52.
29. Buzsaki G, Moser EI. Memory, navigation and theta rhythm in the hippocampal-entorhinal system. Nat Neurosci. 2013; 16:130–8. https://doi.org/10.1038/nn.3304 PMID: 23354386
30. Diehl GW, Hon OJ, Leutgeb S, Leutgeb JK. Grid and Nongrid Cells in Medial Entorhinal Cortex Represent Spatial Location and Environmental Features with Complementary Coding Schemes. Neuron. 2017; 94:83–92. https://doi.org/10.1016/j.neuron.2017.03.004 PMID: 28343867
31. Høydal ØA, Skytøen ER, Moser MB, Moser EI. Object-vector coding in the medial entorhinal cortex. Nature. 2019; Forthcoming.
32. Ezzyat Y, Davachi L. Similarity breeds proximity: pattern similarity within and across contexts is related to later mnemonic judgments of temporal proximity. Neuron. 2014; 81:1176–89.
33. Bornstein AM, Norman KA Reinstated episodic context guides sampling-based decisions for reward. Nat Neurosci. 2017. 20:997–1003. https://doi.org/10.1038/nn.4573 PMID: 28581478
34. Shadlen MN, Shohamy D. Decision Making and Sequential Sampling from Memory. Neuron. 2016; 90:927–39. https://doi.org/10.1016/j.neuron.2016.04.036 PMID: 27253447
35. Bakkour A, Zylberberg A, Shadlen MN, Shohamy D. Value-based decisions involve sequential sampling from memory. bioRxiv. 2018.
36. Maass A, Berron D, Libby LA, Ranganath C, Duzel E. Functional subregions of the human entorhinal cortex. Elife.2015; 4.
37. Navarro Schroeder T, Haak KV, Zaragoza Jimenez NI, Beckmann CF, Doeller CF. Functional topography of the human entorhinal cortex. Elife.2015; 4.
38. Dalton MA, Maguire EA. The pre/parasubiculum: a hippocampal hub for scene-based cognition? Curr Opin Behav Sci. 2017; 17:34–40. https://doi.org/10.1016/j.cobeha.2017.06.001 PMID: 29167810
39. Doeller CF, Barry C, Burgess N. Evidence for grid cells in a human memory network. Nature. 2010; 463:657–61. https://doi.org/10.1038/nature08704 PMID: 20090680
40. Constantinescu AO, O'Reilly JX, Behrens TEJ. Organizing conceptual knowledge in humans with a gridlike code. Science. 2016; 352:1464–68. https://doi.org/10.1126/science.aaf0941 PMID: 27313047
41. Lositsky O, Chen J, Toker D, Honey CJ, Shvartsman M, Poppenk JL, Hasson U, Norman KA Neural pattern change during encoding of a narrative predicts retrospective duration estimates. Elife. 2016; 5.
42. Vass LK, Epstein RA. Common Neural Representations for Visually Guided Reorientation and Spatial Imagery. Cereb Cortex. 2017; 27:1457–71. https://doi.org/10.1093/cercor/bhv343 PMID: 26759482
43. Julian JB, Keinath AT, Frazzetta G, Epstein RA. Human entorhinal cortex represents visual space using a boundary-anchored grid. Nat Neurosci. 2018; 21:191–94. https://doi.org/10.1038/s41593-017-0049-1 PMID: 29311745

44. Meister MLR, Buffalo EA. Neurons in primate entorhinal cortex represent gaze position in multiple spatial reference frames. J Neurosci. 2018, 38:2430–41.

45. Nau M, Navarro Schroeder T, Bellmund JLS, Doeller CF. Hexadirectional coding of visual space in human entorhinal cortex. Nat Neurosci. 2018, 21:188–90. https://doi.org/10.1038/s41593-017-0050-8 PMID: 29311746

46. Dehaene S, Bossini S, Giraux P. The mental representation of parity and number magnitude. Journal of Experimental Psychology: General. 1993, 122:371–96.

47. Dehaene S, Piazza M, Pinel P, Cohen L. Three parietal circuits for number processing. Cognitive Neuropsychology. 2003; 20:487–506. https://doi.org/10.1080/02643290244000239 PMID: 20957581

48. Koenigs M, Barbey AK, Postle BR, Grafman J. Superior parietal cortex is critical for the manipulation of information in working memory. J Neurosci. 2009; 29:14980–14986. https://doi.org/10.1523/JNEUROSCI.3706-09.2009 PMID: 19940193

49. Bueti D, Walsh V. The parietal cortex and the representation of time, space, number and other magnitudes. Philos Trans R Soc Lond B Biol Sci. 2009; 364:1831–40. https://doi.org/10.1098/rstb.2009.0028 PMID: 19487186

50. Doeller CF, Burgess N. Distinct error-correcting and incidental learning of location relative to landmarks and boundaries. Proc Natl Acad Sci USA. 2008; 105:5909–14. https://doi.org/10.1073/pnas.0711433105 PMID: 18413609

51. Doeller CF, King JA, Burgess N. Parallel striatal and hippocampal systems for landmarks and boundaries in spatial memory. Proc Natl Acad Sci USA. 2008; 105:5915–20. https://doi.org/10.1073/pnas.0801489105 PMID: 18408152

52. Vikbladh OM, Meager MR, King J, Blackmon K, Devinsky O, Shohamy D, Burgess N, Daw ND. Hippocampal contributions to model-based planning and spatial memory. Neuron. 2019; Epub

53. Gershman SJ, Daw ND. Reinforcement learning and episodic memory in humans and animals: an integrative framework. Ann Rev Psychol. 2017; 68:101–128.

54. Kosslyn SM. Seeing and imagining in the cerebral hemispheres: A computational approach. Psychological Review, 1987; 94:148–75. PMID: 3575583

55. Baumann O, Mattingley JB. Dissociable roles of the hippocampus and parietal cortex in processing of coordinate and categorical spatial information. Front Hum Neurosci. 2014; 8:73. https://doi.org/10.3389/fnhum.2014.00073 PMID: 24596551

56. Filimon F. Are all spatial reference frames egocentric? Reinterpreting evidence for allocentric, object-centered, or world-centered reference frames. Front Hum Neurosci. 2015; 9:648. https://doi.org/10.3389/fnhum.2015.00648 PMID: 26696861

57. Vann SD, Aggleton JP, Maguire EA. What does the retrosplenial cortex do? Nat Rev Neuro. 2009; 10:792–802.

58. Scalpen KM, Gulati AA, Heimer-McGinn VL, Burwell RD Objects and landmarks: Hippocampal place cells respond differently to manipulations of visual cues depending on size, perspective, and experience. Hippocampus. 2014; 24:1287–99. https://doi.org/10.1002/hipo.22331 PMID: 25045010

59. Epley N, Gilovich T. Putting adjustment back in the anchoring and adjustment heuristic: Differential processing of self-generated and experimenter-provided anchors. Psychol Sci. 2001; 12: 391–96. https://doi.org/10.1111/1467-9280.00372 PMID: 11554672

60. Epley N, Keysar B, Van Boven L, Gilovich T. Perspective tasking as egocentric anchoring and adjustment. J Pers Soc Psychol. 2004; 87:327–39. https://doi.org/10.1037/0022-3514.87.3.327 PMID: 15382983

61. Tamir DI, Mitchell JP. Anchoring and adjustment during social inferences. J Exp Psychol Gen. 2013; 142:151–62. https://doi.org/10.1037/a0028232 PMID: 22506753

62. Tavares RM, Mendelsohn A, Grossman Y, Williams CH, Shapiro M, Trope Y, Schiller D. A Map for Social Navigation in the Human Brain. Neuron. 2015; 87:231–43. https://doi.org/10.1016/j.neuron.2015.06.011 PMID: 26139376

63. Tamir DI, Thornton MA. Modeling the Predictive Social Mind. Trends Cogn Sci. 2018 22:201–12. https://doi.org/10.1016/j.tics.2017.12.005 PMID: 29361382

64. Bellmund JLS, Gardenfors P, Moser EI, Doeller CF. Navigating cognition: Spatial codes for human thinking. Science. 2018; 362.

65. Aronov D, Nevers R, Tank DW. Mapping of a non-spatial dimension by the hippocampal-entorhinal circuit. Nature. 2017; 543:719–22. https://doi.org/10.1038/nature21692 PMID: 28358077

66. Chang SW, Gariepy JF, Platt ML. Neuronal reference frames for social decisions in primate frontal cortex. Nat Neurosci. 2013; 16:243–50. https://doi.org/10.1038/nn.3287 PMID: 23263442

67. Chang SW. Coordinate transformation approach to social interactions. Front Neurosci. 2013; 7: 147. https://doi.org/10.3389/fnins.2013.00147 PMID: 23970850

68. Boorman ED, Rushworth MF, Behrens TE. Ventromedial prefrontal and anterior cingulate cortex adopt choice and default reference frames during sequential multi-alternative choice. J Neurosci, 2013; 33:2242–53. https://doi.org/10.1523/JNEUROSCI.3022-12.2013 PMID: 23392656

69. Shannon CE. A mathematical theory of communication. The Bell System Technical Journal. 1948; 27:379–423.

70. Kaplan R, King J, Koster R, Penny WD, Burgess N, Friston KJ. The neural representation of prospective choice during spatial planning and decisions. PLoS Biol. 2017; 15:e1002588. https://doi.org/10.1371/journal.pbio.1002588 PMID: 28081125

71. Weiskopf N, Hutton C, Josephs O, Deichmann R. Optimal EPI parameters for reduction of susceptibility-induced BOLD sensitivity losses: A whole-brain analysis at 3 T and 1.5 T. Neuroimage. 2006; 33:493–504. https://doi.org/10.1016/j.neuroimage.2006.07.029 PMID: 16959495

72. Brett M, Anton JL, Valabregue R, Poline JB. Region of interest analysis using an SPM toolbox; Sendai, Organization for Human Brain Mapping 2002.

73. Yarkoni T, Poldrack RA, Nichols TE, Van Essen DC, Wager TD. Large-scale automated synthesis of human functional neuroimaging data. Nat Methods. 2011; 8:665–70. https://doi.org/10.1038/nmeth.1635 PMID: 21706013